Equivalent nonlinear beam model for the 3-D analysis of shear-type buildings: application to aeroelastic instability

G. Piccardo[1], F.Tubino[1], A. Luongo[2]

[1]DICCA, Polytechnic School, University of Genoa, Via Montallegro 1, 16145 Genova, Italy
[2] M&MoCS, University of L'Aquila, Zona Ind.le di Bazzano, Loc. Monticchio, 67100 L'Aquila, Italy
email: giuseppe.piccardo@unige.it, federica.tubino@unige.it, angelo.luongo@univaq.it

Cite this article as: Piccardo G., Tubino F., Luongo A. Equivalent nonlinear beam model for the 3-D analysis of shear-type buildings: application to aeroelastic instability. *International Journal of Non-Linear Mechanics* 80 (2016) 52-65

ABSTRACT: Tower buildings can be very sensitive to dynamic actions and their dynamic analysis is usually carried out numerically through sophisticated finite element models. In this paper, an equivalent nonlinear one-dimensional shear-shear-torsional beam model immersed in a three-dimensional space is introduced to reproduce, in an approximate way, the dynamic behavior of tower buildings. It represents an extension of a linear beam model recently introduced by the authors, accounting for nonlinearities generated by the stretching of the columns. The constitutive law of the beam is identified from a discrete model of a 3D-frame, via a homogenization process, which accounts for the rotation of the floors around the tower axis. The macroscopic shear strain in the equivalent beam is produced by the bending of columns, accompanied by negligible rotation of the floors. A coupled nonlinear shear-torsional mechanical model is thus obtained. The coupling between shear and torsion is related to a non-symmetric layout of the columns, while mechanical nonlinearities are proportional to the slenderness of the columns. The model can be used for the analysis of the response of tower buildings to any kind of dynamic and static excitation. A first application is here presented, to investigate the effect of mechanical and aerodynamic coupling on the critical galloping conditions and on the postcritical behavior of tower buildings, based on a quasi-steady model of aerodynamic forces.

KEY WORDS: Equivalent beam model, Homogenization procedure, Nonlinear beam model, Perturbation approach, Shear-type building.

1 INTRODUCTION

Tower buildings are very sensitive to dynamic actions induced by wind and earthquake. Simplified one-dimensional beam models can be very useful at a preliminary design stage. The continuum approach generally proves to be simple, and it can provide reasonable results with significantly reduced computing time with respect to refined numerical models. In addition, in certain cases, good preliminary hand estimates can be done without much difficulty and general parametric studies can be easily performed.

The possibility of adopting equivalent one-dimensional coarse models representative of the global behavior of different kinds of three-dimensional systems is deeply analyzed in [1]. In the analysis of tall buildings subjected to lateral loads, different models have been proposed in the literature idealizing the structure as a beam with continuum properties along its height. Basu and Dar [2] determined the dynamic characteristics (natural frequencies and mode shapes) of multistory buildings idealized as an equivalent planar coupled shear wall connected in series to an equivalent frame: they modelled the coupled wall as a continuum of uniform properties and the frame as a uniform shear beam. Balendra et al [3] analyzed a completely asymmetric building through an equivalent beam model with in parallel arrangement of bending and shear stiffness, using a Galerkin technique in the continuum approach. Chajes at al [4] introduced a plane equivalent Timoshenko beam model with an additional degree of freedom, whose properties are determined from the equivalence of the strain energy of the continuum and the discrete model. Miranda and Taghavi [5] introduced an approximate method to estimate floor acceleration demands in multistory buildings: the dynamic characteristics of the building are approximated by using a simplified model based on an equivalent beam that consists of a combination of a flexural and a shear beam. Malekinejad and Rahgozar [6] provided approximate formulas for the modal properties of tubular tall building structures, considering a parallel cantilevered flexural-shear beam and deriving the governing dynamic equation using the energy method and Hamilton’s principle. Cluni et al [7]

proposed two plane equivalent beam models, using in series and in parallel arrangement of the bending and shear stiffness, in order to estimate the dynamic wind-excited response of tall buildings: the parameters of the mechanical model are calibrated using equivalence criteria based on static and dynamic response features of finite element models.

The equivalent beam models proposed in the literature are mainly limited to the representation of the lateral behavior of tall buildings, neglecting the coupling between shear and torsion components of the motion. However, as described many times in the technical literature, the coupling between shear and torsion may be important in the determination of the wind-excited response (e.g. [8], [9], [10]). Concerning shear-type buildings, the authors have recently introduced a continuous one-dimensional equivalent beam model immersed in a three-dimensional space, that allows to take into account also the coupling between the two shear components and the torsion around the beam axis [11]. In this model, the macroscopic shear strain is produced by bending of the columns, accompanied by negligible rotation of rigid floors, prevented by the high axial stiffness of the columns. The torsional effect induced by the rotation of the floors around the tower axis is also included.

In this paper, the linear model introduced in [11] through a heuristic identification method (similarly to, e.g., [12],[13]) is extended, taking into account the nonlinearities generated by the stretch of the columns. In a way similar to [4], based on the equivalence between the elastic energy of the building and of the equivalent beam model, a constitutive law is introduced relating the internal forces to the three strain components. However, differently from [4] and [11], the equivalent model here proposed is nonlinear and it allows to consider the intrinsic mechanical coupling between torsion and shear, related to a generic non-symmetric positioning of the columns. The introduced model can be applied to evaluate the response of shear-type buildings to dynamic actions of different nature (e.g., earthquake, wind). In this paper, a preliminary application to an ideal square building with non-symmetrically disposed columns subjected to wind excitation is

proposed. The effect of the coupling between shear and torsion on the galloping critical condition is studied. Furthermore, the influence of the aerodynamic and mechanical nonlinearities on the galloping post-critical oscillation amplitude is analyzed.

2 SHEAR-BEAM MODEL: KYNEMATICS

A shear-beam is characterized by shear strains much larger than flexural ones: it is a coarse model for shear-type frames under planar excitation transverse to the axis. The beam is considered as a one-dimensional polar continuum whose points, in the reference configuration, lie on the segment $s\in[0,\ell]$ (assumed to be coincident with the *centroidal axis* of the underlying three-dimensional model). The beam is endowed with a rigid local structure, described by mutually orthogonal unit vectors attached to the material points. Let $\bar{\mathbf{a}}_1$, $\bar{\mathbf{a}}_2$, $\bar{\mathbf{a}}_3$ be the triad in the reference configuration, with $\bar{\mathbf{a}}_1$ aligned on the beam axis (Fig. 1), and let $\mathbf{a}_1(s,t)$, $\mathbf{a}_2(s,t)$, $\mathbf{a}_3(s,t)$ be the transformed triad in the current configuration, occupied at time t (Fig. 2). The beam is assumed internally constrained, namely unflexurable and clamped at one end. Therefore $\bar{\mathbf{a}}_1\equiv\mathbf{a}_1$ and $\mathbf{a}_2=\bar{\mathbf{a}}_2\cos\theta+\bar{\mathbf{a}}_3\sin\theta$, $\mathbf{a}_3=-\bar{\mathbf{a}}_2\sin\theta+\bar{\mathbf{a}}_3\cos\theta$, where θ is the *twist* angle. Consequently, the current configuration of the beam is described by four scalar configuration variables, the displacement of the centroidal axis $\mathbf{u}:=u_1(s,t)\,\bar{\mathbf{a}}_1+u_2(s,t)\,\bar{\mathbf{a}}_2+u_3(s,t)\,\bar{\mathbf{a}}_3$ and the twist $\theta(s,t)$ (Fig. 2).

The vectors $\mathbf{e}:=\mathbf{R}^{\mathrm{T}}\mathbf{u}'$, $\boldsymbol{\kappa}:=\theta'(s,t)\bar{\mathbf{a}}_1$, where $\mathbf{R}$ represents the rotation tensor around $\bar{\mathbf{a}}_1$ and the dash denotes differentiation with respect to s, are defined as the *strain vector* and *torsion*, respectively; moreover, $\mathbf{e}:=\varepsilon\bar{\mathbf{a}}_1+\boldsymbol{\gamma}$, ε being the axial and $\boldsymbol{\gamma}$ the shear strain. By letting $\boldsymbol{\gamma}:=\gamma_2\,\bar{\mathbf{a}}_2+\gamma_3\,\bar{\mathbf{a}}_3$, $\boldsymbol{\kappa}:=\kappa_t\,\bar{\mathbf{a}}_1$, their scalar components in the current configurations are:

$$\begin{aligned}
\varepsilon &= u_1' \\
\gamma_2 &= u_2'\cos\theta + u_3'\sin\theta \\
\gamma_3 &= -u_2'\sin\theta + u_3'\cos\theta \\
\kappa_t &= \theta'
\end{aligned} \tag{1}$$

Geometrical boundary conditions at the clamped end *D* require:

$$u_{1D} = u_{2D} = u_{3D} = \theta_D = 0 \tag{2}$$

3 SHEAR-BEAM MODEL: DYNAMICS

External forces $\mathbf{p}:= p_2(s,t)\,\bar{\mathbf{a}}_2 + p_3(s,t)\,\bar{\mathbf{a}}_3$ and couples $\mathbf{c}:=c(s,t)\,\bar{\mathbf{a}}_1$ are acting on the beam (Fig. 1). The internal contact force $\mathbf{t}:= N(s,t)\mathbf{a}_1+T_2(s,t)\mathbf{a}_2+T_3(s,t)\mathbf{a}_3$ and the couple $\mathbf{m}:=M_t\mathbf{a}_1$ are assumed as stress measures, and referred as the *stress force* (composed of the normal N and shear force T_2, T_3 components) and the *torsional moment* M_t. Equilibrium in the current configuration, requires $\mathbf{t}'+\mathbf{p}=\mathbf{0}$ and $\mathbf{m}'+(\bar{\mathbf{a}}_1+\mathbf{u}')\times\mathbf{t}+\mathbf{c}=\mathbf{0}$ [1]. When forces are projected onto the reference configuration, the scalar balance equations read:

$$\begin{aligned}
&N' + p_1 = 0 \\
&\left(T_2\cos\theta - T_3\sin\theta\right)' + p_2 = 0 \\
&\left(T_2\sin\theta + T_3\cos\theta\right)' + p_3 = 0 \\
&M_t' + T_2\left(u_2'\sin\theta - u_3'\cos\theta\right) + T_3\left(u_2'\cos\theta + u_3'\sin\theta\right) + c = 0
\end{aligned} \tag{3}$$

The mechanical boundary conditions, to be satisfied at the free end *E*, are:

$$\begin{aligned}
&N_{1E} - P_{1E} = 0 \\
&T_{2E}\cos\theta_E - T_{3E}\sin\theta_E - P_{2E} = 0 \\
&T_{2E}\sin\theta_E + T_{3E}\cos\theta_E - P_{3E} = 0 \\
&M_{tE} - C_E = 0
\end{aligned} \tag{4}$$

where $\mathbf{P}_E:= P_{1E}(t)\,\bar{\mathbf{a}}_1 + P_{2E}(t)\,\bar{\mathbf{a}}_2 + P_{3E}(t)\,\bar{\mathbf{a}}_3$ and $\mathbf{C}_E:=C_E(t)\,\bar{\mathbf{a}}_1$ are possible (known) forces and couple, respectively, dynamically acting in *E*.

4 SHEAR-BEAM MODEL: HYPERELASTIC LAW

A nonlinear hyperelastic law is introduced starting from an expression of the density of elastic potential energy that takes into account the stretching of the single columns. In order to account for the stretching effect, an axial displacement of columns is allowed to occur. This, however, is condensed by requiring that the resulting axial force is zero. The condition entails that, in the fine model, when a floor rotates with respect to an adjacent one, columns undergo axial strains, which depend on their position with respect the center of rotation; therefore, axial forces arise. Their sum, however, must be zero, and then a *shortening* of the inter-story distance occurs. For this fact, although the resultant of the axial forces is zero, an elastic energy is stored in the cell due to the stretching of the single columns.

In this section, at first a single column is analyzed (Section 4.1). Then, a cell made of two adjacent floors is considered (Section 4.2) and, by enforcing that the resulting axial force is zero, a relationship between the axial displacement (slave variable) and the transverse displacement and twist of the floor is obtained. Thus, starting from the density of elastic potential energy, the nonlinear elastic law is derived by the Green law (Section 4.3).

4.1 Single column analysis

Let us consider a column *c* of longitudinal axis $\bar{\mathbf{a}}_1$, and principal inertia axes $\bar{\mathbf{a}}_2, \bar{\mathbf{a}}_3$, clamped at both ends *C* and *B*, undergoing a displacement $\mathbf{u}_B = u_{1B}\bar{\mathbf{a}}_1 + u_{2B}\bar{\mathbf{a}}_2 + u_{3B}\bar{\mathbf{a}}_3$ and a twist θ_B, assigned at *B* (Fig. 3). In the framework of the linear theory, the column experiences a displacement field:

$$\mathbf{u}(s) = u_{1B} g(s) \bar{\mathbf{a}}_1 + f(s)\left(u_{2B}\bar{\mathbf{a}}_2 + u_{3B}\bar{\mathbf{a}}_3\right) \tag{5}$$

where *s* is an abscissa with origin at *C*, and the functions *g* and *f* are given by:

$$g(s) := s/h \qquad\qquad f(s) := 3(s/h)^2 - 2(s/h)^3 \tag{6}$$

h being the length of the column. Based on a perturbation approach, we substitute this first-order solution in the expression for the (truncated) axial strain ε_c, and we find:

$$\varepsilon_c(s) = u_1'(s) + \frac{1}{2}\left(u_2'^2(s) + u_3'^2(s)\right) = u_{1B}g'(s) + \frac{1}{2}\left(u_{2B}^2 + u_{3B}^2\right) f'^2(s) \tag{7}$$

Substitution of Eq. (6) into Eq. (7) and integration on the domain [C, B], provides the axial strain:

$$\varepsilon_c(s) = \frac{u_{1B}}{h} + \frac{1}{2}\frac{\left(u_{2B}^2 + u_{3B}^2\right)}{h^2}\left(6\frac{s}{h} - 6\frac{s^2}{h^2}\right)^2 \tag{8}$$

The elastic energy stored by the generic column can be expressed as the sum of the flexural-torsional U_c^{ft} and axial U_c^a contributions as follows:

$$U_c = U_c^{ft} + U_c^a \tag{9}$$

where the two contributions are given by:

$$\begin{aligned} U_c^{ft} &:= \frac{1}{2}\left(k_{2c}^f u_{2B}^2 + k_{3c}^f u_{3B}^2 + k_c^t \theta_B^2\right) \\ U_c^a &:= \frac{1}{2}\int_0^h EA\varepsilon_c(s)^2 \,\mathrm{d}s = \frac{1}{2}k_c^a\left[u_{1B}^2 + \frac{18}{35}\frac{\left(u_{2B}^2 + u_{3B}^2\right)^2}{h^2} + \frac{6}{5}\left(u_{2B}^2 + u_{3B}^2\right)\frac{u_{1B}}{h}\right] \end{aligned} \tag{10}$$

where $k_{2c}^f := 12EI_{3c}/h^3$; $k_{3c}^f := 12EI_{2c}/h^3$ are flexural stiffnesses, $k_c^t := GJ_t/h$ is the torsional stiffness, and $k_c^a := EA/h$ is the axial stiffness. The energy is, therefore, quartic in the displacements.

It should be noted that, in order the column experiences the assigned displacements, not only moments and shear forces are needed at the ends, but also the axial force:

$$N_c = \frac{\partial U_c}{\partial u_{1B}} = k_c^a\left[u_{1B} + \frac{3}{5h}\left(u_{2B}^2 + u_{3B}^2\right)\right] \tag{11}$$

4.2 Cell analysis

Let us consider a cell made of two adjacent floors, parallel to the $\bar{\mathbf{a}}_2, \bar{\mathbf{a}}_3$ plane, connected by N columns of equal height h aligned along $\bar{\mathbf{a}}_1$. Let us consider the relative motion of the upper floor with respect to the lower, consisting in a translation $\mathbf{u}_G = u_{1G}\bar{\mathbf{a}}_1 + u_{2G}\bar{\mathbf{a}}_2 + u_{3G}\bar{\mathbf{a}}_3$, G being the centroid, and in a rotation θ around the axis $\bar{\mathbf{a}}_1$. Using a linear kinematics since the twist angle θ is generally small, the displacement of the top point of the i-th column, of coordinates x_{2i}, x_{3i}, is $\mathbf{u}_i = u_{1i}\bar{\mathbf{a}}_1 + u_{2i}\bar{\mathbf{a}}_2 + u_{3i}\bar{\mathbf{a}}_3$, where:

$$\begin{aligned} u_{1i} &= u_{1G} \\ u_{2i} &= u_{2G} - \theta x_{3i} \\ u_{3i} &= u_{3G} + \theta x_{2i} \end{aligned} \tag{12}$$

Assuming that all the columns have principal axes aligned with $\bar{\mathbf{a}}_2, \bar{\mathbf{a}}_3$, the total elastic energy of the N columns can be expressed as:

$$U := \sum_{i=1}^{N} U_i \tag{13}$$

where U_i represents the elastic energy of the i-th column. Substituting Eqs. (9)-(10) (by replacing subscripts c and B with the new generic one i) into Eq. (13), the elastic energy of the cell is given by:

$$U := \frac{1}{2}\sum_{i=1}^{N}\left\{ k_{2i}^{f} u_{2i}^{2} + k_{3i}^{f} u_{3i}^{2} + k_i^{t}\theta^2 + k_i^{a}\left[u_{1i}^{2} + \frac{18}{35}\frac{\left(u_{2i}^{2} + u_{3i}^{2}\right)^2}{h^2} + \frac{6}{5}\left(u_{2i}^{2} + u_{3i}^{2}\right)\frac{u_{1i}}{h} \right] \right\} \tag{14}$$

Then, substituting Eq. (12) into Eq. (14), one obtains the following expression of the elastic energy U as a function of the displacements of the centroid (u_{1G}, u_{2G}, u_{3G}) and of the rotation θ:

$$U=\frac{1}{2}\left\{\begin{array}{l}\sum_{i=1}^{N}\left[k_{2i}^{f}\left(u_{2G}-\theta x_{3i}\right)^{2}+k_{3i}^{f}\left(u_{3G}+\theta x_{2i}\right)^{2}+k_{i}^{t}\theta^{2}\right]+\\ \sum_{i=1}^{N}k_{i}^{a}\left[u_{1G}^{2}+\frac{18}{35}\frac{\left(\left(u_{2G}-\theta x_{3i}\right)^{2}+\left(u_{3G}+\theta x_{2i}\right)^{2}\right)^{2}}{h^{2}}+\frac{6}{5}\left(\left(u_{2G}-\theta x_{3i}\right)^{2}+\left(u_{3G}+\theta x_{2i}\right)^{2}\right)\frac{u_{1G}}{h}\right]\end{array}\right\} \quad (15)$$

The axial force necessary to enforce such displacements is:

$$N=\frac{\partial U}{\partial u_{1G}}=\sum_{i=1}^{N}k_{i}^{a}\left[u_{1G}+\frac{3}{5h}\left(u_{2G}-\theta x_{3i}\right)^{2}+\frac{3}{5h}\left(u_{3G}+\theta x_{2i}\right)^{2}\right] \quad (16)$$

If no axial forces are applied, then $N = 0$, and therefore the centroidal axial displacement can be obtained as slave of the centroidal transversal displacements and of the twist:

$$u_{1G}=-\frac{3}{5h}\left(u_{2G}^{2}+u_{3G}^{2}+\rho^{2}\theta^{2}-2x_{3A}u_{2G}\theta+2x_{2A}u_{3G}\theta\right) \quad (17)$$

where ρ^2 is the squared polar inertia radius of the *axial* stiffnesses with respect to the centroid, x_{2A} and x_{3A} are the coordinates of the center *A* of the *axial* stiffness (generally *A* does not coincide with the flexural center *F*), given by:

$$\rho^{2}:=\frac{1}{K^{a}}\sum_{j=1}^{N}k_{j}^{a}\left(x_{2j}^{2}+x_{3j}^{2}\right) \qquad x_{2A}:=\frac{1}{K^{a}}\sum_{j=1}^{N}k_{j}^{a}x_{2j} \qquad x_{3A}:=\frac{1}{K^{a}}\sum_{j=1}^{N}k_{j}^{a}x_{3j} \quad (18)$$

being $K^{a}:=\sum_{j=1}^{N}k_{j}^{a}$ the total axial stiffness.

By substituting u_{1G} given by Eq. (17) into Eq. (15), the passive variable u_{1G} is eliminated, and we obtain:

$$U=\frac{1}{2}\left\{\begin{array}{l}\displaystyle\sum_{i=1}^{N}\left[k_{2i}^{f}\left(u_{2G}-\theta x_{3i}\right)^2+k_{3i}^{f}\left(u_{3G}+\theta x_{2i}\right)^2+k_i^t\theta^2\right]+\\ \displaystyle\sum_{i=1}^{N}k_i^a\left[\begin{array}{l}\left[-\frac{3}{5h}\left(u_{2G}^2+u_{3G}^2+\rho^2\theta^2-2x_{3A}u_{2G}\theta+2x_{2A}u_{3G}\theta\right)\right]^2+\\ +\frac{18}{35}\frac{\left(\left(u_{2G}-\theta x_{3i}\right)^2+\left(u_{3G}+\theta x_{2i}\right)^2\right)^2}{h^2}+\\ +\frac{6}{5h}\left(\left(u_{2G}-\theta x_{3i}\right)^2+\left(u_{3G}+\theta x_{2i}\right)^2\right)\left[-\frac{3}{5h}\left(u_{2G}^2+u_{3G}^2+\rho^2\theta^2-2x_{3A}u_{2G}\theta+2x_{2A}u_{3G}\theta\right)\right]\end{array}\right]\end{array}\right\} \quad (19)$$

The second term in the sum of Eq. (19) is the axial contribution to the elastic potential energy of the cell: it is a 4-degree homogeneous polynomial.

4.3 Constitutive law identification

Let us assume that the strain components are constant along the interstorey distance h. The constitutive law of the coarse model is obtained by expressing the centroid displacements through the (constant) admissible strains:

$$u_{2G}=\gamma_2 h \quad u_{3G}=\gamma_3 h \quad \theta=\kappa_t h \quad (20)$$

The elastic energy per unit length of the equivalent beam is thus simply deduced by the elastic energy of the cell, $\phi=U/h$. By substituting Eq.(20) into Eq. (19), we obtain:

$$\phi=\frac{h}{2}\left\{\begin{array}{l}\displaystyle\sum_{i=1}^{N}\left[k_{2i}^{f}\left(\gamma_2-\kappa_t x_{3i}\right)^2+k_{3i}^{f}\left(\gamma_3+\kappa_t x_{2i}\right)^2+k_i^t\kappa_t^2\right]+\\ \displaystyle\sum_{i=1}^{N}k_i^a\left[\begin{array}{l}\left[-\left(\gamma_2^2+\gamma_3^2+\rho^2\kappa_t^2-2x_{3A}\gamma_2\kappa_t+2x_{2A}\gamma_3\kappa_t\right)\right]^2+\\ +\frac{18}{35}\left(\left(\gamma_2-\kappa_t x_{3i}\right)^2+\left(\gamma_3+\kappa_t x_{2i}\right)^2\right)^2+\\ +\frac{6}{5}\left(\left(\gamma_2-\kappa_t x_{3i}\right)^2+\left(\gamma_3+\kappa_t x_{2i}\right)^2\right)\left[-\frac{3}{5}\left(\gamma_2^2+\gamma_3^2+\rho^2\kappa_t^2-2x_{3A}\gamma_2\kappa_t+2x_{2A}\gamma_3\kappa_t\right)\right]\end{array}\right]\end{array}\right\} \quad (21)$$

By the Green law

$$T_2=\frac{\partial\phi}{\partial\gamma_2},\quad T_3=\frac{\partial\phi}{\partial\gamma_3},\quad M_t=\frac{\partial\phi}{\partial\kappa_t} \tag{22}$$

a constitutive law is obtained:

$$\begin{aligned}
T_2&=hK_2^f\gamma_2-hx_{3F}K_2^f\kappa_t+\delta\begin{pmatrix}C_{2222}\gamma_2^3+C_{2333}\gamma_3^3+C_{2ttt}\kappa_t^3+C_{2223}\gamma_2^2\gamma_3+C_{222t}\gamma_2^2\kappa_t+\\+C_{2332}\gamma_3^2\gamma_2+C_{233t}\gamma_3^2\kappa_t+C_{2tt2}\kappa_t^2\gamma_2+C_{2tt3}\kappa_t^2\gamma_3+C_{223t}\gamma_2\gamma_3\kappa_t\end{pmatrix}\\
T_3&=hK_3^f\gamma_3+hx_{2F}K_3^f\kappa_t+\delta\begin{pmatrix}C_{3222}\gamma_2^3+C_{3333}\gamma_3^3+C_{3ttt}\kappa_t^3+C_{3223}\gamma_2^2\gamma_3+C_{322t}\gamma_2^2\kappa_t+\\+C_{3332}\gamma_3^2\gamma_2+C_{333t}\gamma_3^2\kappa_t+C_{3tt2}\kappa_t^2\gamma_2+C_{3tt3}\kappa_t^2\gamma_3+C_{323t}\gamma_2\gamma_3\kappa_t\end{pmatrix}\\
M_t&=h\left(K^t+K^{tf}\right)\kappa_t-hx_{3F}K_2^f\gamma_2+hx_{2F}K_3^f\gamma_3+\delta\begin{pmatrix}C_{t222}\gamma_2^3+C_{t333}\gamma_3^3+C_{tttt}\kappa_t^3+C_{t223}\gamma_2^2\gamma_3+C_{t22t}\gamma_2^2\kappa_t+\\+C_{t332}\gamma_3^2\gamma_2+C_{t33t}\gamma_3^2\kappa_t+C_{ttt2}\kappa_t^2\gamma_2+C_{ttt3}\kappa_t^2\gamma_3+C_{t23t}\gamma_2\gamma_3\kappa_t\end{pmatrix}
\end{aligned} \tag{23}$$

characterized by a linear and a nonlinear (cubic) part, which accounts for pure torsion, pure shear and coupling between shear and torsion.

In Eq. (23), $K_2^f:=\sum_{i=1}^N k_{2i}^f$ and $K_3^f:=\sum_{i=1}^N k_{3i}^f$ are the total flexural stiffnesses, $K^t:=\sum_{i=1}^N k_i^t$ is the total torsional stiffness, $K^{tf}:=\sum_{i=1}^N\left(k_{2i}^f x_{3i}^2+k_{3i}^f x_{2i}^2\right)$ is the contribution to the torsional stiffness given by the flexural stiffness of the columns, and $\delta:=18/175K^a h$; x_{2F} and x_{3F} are the coordinates of the center F of the flexural stiffness:

$$x_{2F}:=\frac{1}{K_3^f}\sum_{i=1}^N k_{3i}^f x_{2i}\qquad x_{3F}:=\frac{1}{K_2^f}\sum_{i=1}^N k_{2i}^f x_{3i} \tag{24}$$

The explicit expression of coefficients of the cubic terms in Eq. (23) are given in Appendix A.

5 THE FUNDAMENTAL PROBLEM

The fundamental problem is governed by the kinematic relationships (1), (2), the balance equations (3), (4), and the elastic law (23). External forces are in general given by the sum of inertial, damping and aerodynamic terms:

$$\begin{aligned}
&\mathbf{p} = \mathbf{p}_a - m\ddot{\mathbf{u}} - \xi_u \dot{\mathbf{u}} \\
&\mathbf{c} = \mathbf{c}_a - I_1 \ddot{\theta}\bar{\mathbf{a}}_1 - \xi_\theta \dot{\theta}\bar{\mathbf{a}}_1 \\
&\mathbf{P}_E = \mathbf{P}_{Ea} - M_E \ddot{\mathbf{u}}_E - \Xi_{uE}\dot{\mathbf{u}}_E \\
&\mathbf{C}_E = \mathbf{C}_{Ea} - \left(I_{1E}\ddot{\theta}_E - \Xi_{\theta E}\dot{\theta}_E\right)\bar{\mathbf{a}}_1
\end{aligned} \tag{25}$$

where the index *a* denotes aerodynamic; *m* is the mass per unit length of the beam; I_1 is the inertia mass moment of the cross section with respect to $\bar{\mathbf{a}}_1$; M_E is a lumped mass, possibly attached at the free end of the beam, and I_{1E} its inertia moment. *External* damping forces are taken proportional to the masses, via the damping coefficients ξ, Ξ; internal damping, if any, must be accounted via a visco-elastic constitutive law. Note that the centroidal axis was taken as the beam axis in order to simplify the expression of the inertia forces.

The general form of the equations of motion becomes:

$$\begin{aligned}
&hK_2^f u_2'' - hx_{3F}K_2^f\theta'' + \delta\begin{pmatrix} C_{2222}u_2'^3 + C_{2333}u_3'^3 + C_{2ttt}\theta'^3 + C_{2223}u_2'^2u_3' + C_{222t}u_2'^2\theta' + \\ + C_{2332}u_3'^2u_2' + C_{233t}u_3'^2\theta' + C_{2tt2}\theta'^2u_2' + C_{2tt3}\theta'^2u_3' + C_{223t}u_2'u_3'\theta' \end{pmatrix} + \\
&\qquad + p_{a2} - m\ddot{u}_2 - c_2\dot{u}_2 = 0 \\
&hK_3^f u_3'' + hx_{2F}K_3^f\theta'' + \delta\begin{pmatrix} C_{3222}u_2'^3 + C_{3333}u_3'^3 + C_{3ttt}\theta'^3 + C_{3223}u_2'^2u_3' + C_{322t}u_2'^2\theta' + \\ + C_{3332}u_3'^2u_2' + C_{333t}u_3'^2\theta' + C_{3tt2}\theta'^2u_2' + C_{3tt3}\theta'^2u_3' + C_{323t}u_2'u_3'\theta' \end{pmatrix} + \\
&\qquad + p_{a3} - m\ddot{u}_3 - c_3\dot{u}_3 = 0 \\
&h\left(K^t + K^{tf}\right)\theta'' - hx_{3F}K_2^f u_2'' + hx_{2F}K_3^f u_3'' + \\
&+\delta\begin{pmatrix} C_{t222}u_2'^3 + C_{t333}u_3'^3 + C_{tttt}\theta'^3 + C_{t223}u_2'^2u_3' + C_{t22t}u_2'^2\theta' + \\ + C_{t332}u_3'^2u_2' + C_{t33t}u_3'^2\theta' + C_{ttt2}\theta'^2u_2' + C_{ttt3}\theta'^2u_3' + C_{t23t}u_2'u_3'\theta' \end{pmatrix} + c_a - I_1\ddot{\theta} - c_\theta\dot{\theta} = 0
\end{aligned} \tag{26}$$

In absence of external applied forces at the free end *E*, the boundary conditions are given by:

$$
\begin{aligned}
&u_2(0)=u_3(0)=\theta(0)=0\\
&hK_2^f u_2'(\ell)-hx_{3F}K_2^f\theta'(\ell)=0\\
&hK_3^f u_3'(\ell)+hx_{2F}K_3^f\theta'(\ell)=0\\
&h\left(K^t+K^{tf}\right)\theta'(\ell)-hx_{3F}K_2^f u_2'(\ell)+hx_{2F}K_3^f u_3'(\ell)=0
\end{aligned}
\tag{27}
$$

Drawing inspiration from the exact solution of the mechanically linear system [11], we can follow a Galerkin approach to solve the boundary value problem (26)-(27) by taking:

$$
\begin{aligned}
u_2(s,t)&=\sin\left(\frac{\pi}{2}\frac{s}{l}\right)q_2(t)\\
u_3(s,t)&=\sin\left(\frac{\pi}{2}\frac{s}{l}\right)q_3(t)\\
\theta(s,t)&=\sin\left(\frac{\pi}{2}\frac{s}{l}\right)q_t(t)
\end{aligned}
\tag{28}
$$

where q_2, q_3, q_t are unknown amplitudes. Introducing the nondimensional parameters:

$$
\begin{aligned}
&\tilde{t}=\omega_3 t,\ \tilde{q}_2=\frac{q_2}{b},\ \tilde{q}_3=\frac{q_3}{b},\ \tilde{q}_t=q_t,\ \xi_2=\frac{c_2}{2m\omega_2},\ \xi_3=\frac{c_3}{2m\omega_3},\\
&\xi_\theta=\frac{c_\theta}{2I_1\omega_\theta},\ \tilde{x}_{2F}=\frac{x_{2F}}{b},\ \tilde{x}_{3F}=\frac{x_{3F}}{b},\ \alpha_{23}=\frac{\omega_2}{\omega_3},\ \alpha_{\theta 3}=\frac{\omega_\theta}{\omega_3},\\
&\eta=\frac{I_1}{mb^2},\quad \alpha_1=-\frac{27}{200}\pi^2\frac{\lambda_c^2}{\lambda^2},\ \lambda_c=\frac{1}{\sqrt{12}}\frac{h}{\rho_{2c}},\ \lambda=\frac{\ell}{b}
\end{aligned}
\tag{29}
$$

λ_c and λ being related to the slenderness of the column and of the tower building, respectively, ρ_{2c} being the radius of inertia of the section of the column with respect to x_2 axis, ω_2, ω_3 and ω_θ the circular frequencies of the building in the uncoupled case (i.e., symmetrical cross-section with respect to the reference axes; [14]),

$$
\omega_2^2=\frac{hK_2^f}{m}\left(\frac{\pi}{2\ell}\right)^2,\ \omega_3^2=\frac{hK_3^f}{m}\left(\frac{\pi}{2\ell}\right)^2,\ \omega_\theta^2=\frac{h\left(K^t+K^{tf}\right)}{I_1}\left(\frac{\pi}{2\ell}\right)^2
\tag{30}
$$

the resulting non-dimensional system of second-order ordinary differential equations can be written in the following synthetic matrix form:

$$\mathbf{M}\ddot{\tilde{\mathbf{q}}}+\mathbf{C}_s\dot{\tilde{\mathbf{q}}}+\mathbf{K}_s\tilde{\mathbf{q}}=\mathbf{f}_1\left(\tilde{\mathbf{q}},\dot{\tilde{\mathbf{q}}};\mu\right)+\mathbf{f}_2\left(\tilde{\mathbf{q}},\dot{\tilde{\mathbf{q}}};\mu\right)+\mathbf{f}_3\left(\tilde{\mathbf{q}},\dot{\tilde{\mathbf{q}}};\mu\right) \tag{31}$$

where $\tilde{\mathbf{q}}$ is the vector of the non-dimensional principal coordinates, μ is a suitable control parameter, $\mathbf{f}_k$ (k=1,2,3) are homogenous polynomials of k-degree in $\tilde{\mathbf{q}}, \dot{\tilde{\mathbf{q}}}$ and their combinations, also depending from the parameter μ, and $\mathbf{M}$, $\mathbf{C}_s$, $\mathbf{K}_s$ are the structural mass, damping and stiffness matrixes,

$$\tilde{\mathbf{q}}=\begin{Bmatrix}\tilde{q}_2\\ \tilde{q}_3\\ \tilde{q}_t\end{Bmatrix} \quad \mathbf{M}=\begin{bmatrix}1&0&0\\0&1&0\\0&0&\eta\end{bmatrix} \quad \mathbf{C}_s=\begin{bmatrix}2\xi_2\alpha_{23}&0&0\\0&2\xi_3&0\\0&0&2\xi_\theta\alpha_{\theta 3}\eta\end{bmatrix} \quad \mathbf{K}_s=\begin{bmatrix}\alpha_{23}^2&0&-\tilde{x}_{3F}\alpha_{23}^2\\0&1&\tilde{x}_{2F}\\-\tilde{x}_{3F}\alpha_{23}^2&\tilde{x}_{2F}&\alpha_{\theta 3}^2\eta\end{bmatrix} \tag{32}$$

Specifying the aerodynamic forces to the self-excited aeroelastic case through a quasi-steady approach [11], the linear vector $\mathbf{f}_1$ is expressed as a function of the aerodynamic damping and stiffness matrixes:

$$\mathbf{f}_1\left(\tilde{\mathbf{q}},\dot{\tilde{\mathbf{q}}};\mu\right)=-\mu\mathbf{C}_a\dot{\tilde{\mathbf{q}}}-\mu^2\mathbf{K}_a\tilde{\mathbf{q}} \tag{33}$$

where μ is the nondimensional (reduced) mean wind velocity, $\mu=U/(\omega_3 b)$. The explicit expression of these matrices, together with that of the aerodynamic forces p_{a2}, p_{a3}, c_a, is given in Appendix B. Therefore, in this case, the nonlinear vectors $\mathbf{f}_2$ and $\mathbf{f}_3$ are the following quadratic (aerodynamic) and cubic (aerodynamic and mechanical) force vectors:

$$\mathbf{f}_2\left(\tilde{\mathbf{q}},\dot{\tilde{\mathbf{q}}};\mu\right)=\frac{8}{3\pi}\nu\begin{Bmatrix} C_{a222}\dot{\tilde{q}}_2^2+C_{a233}\dot{\tilde{q}}_3^2+\mu^2C_{a2tt}\tilde{q}_t^2+\mu C_{a22t}\dot{\tilde{q}}_2\tilde{q}_t+\mu C_{a23t}\dot{\tilde{q}}_3\tilde{q}_t+C_{a223}\dot{\tilde{q}}_2\dot{\tilde{q}}_3 \\ C_{a322}\dot{\tilde{q}}_2^2+C_{a333}\dot{\tilde{q}}_3^2+\mu^2C_{a3tt}\tilde{q}_t^2+\mu C_{a32t}\dot{\tilde{q}}_2\tilde{q}_t+\mu C_{a33t}\dot{\tilde{q}}_3\tilde{q}_t+C_{a323}\dot{\tilde{q}}_2\dot{\tilde{q}}_3 \\ C_{at22}\dot{\tilde{q}}_2^2+C_{at33}\dot{\tilde{q}}_3^2+\mu^2C_{attt}\tilde{q}_t^2+\mu C_{at2t}\dot{\tilde{q}}_2\tilde{q}_t+\mu C_{at3t}\dot{\tilde{q}}_3\tilde{q}_t+C_{at23}\dot{\tilde{q}}_2\dot{\tilde{q}}_3 \end{Bmatrix}$$

$$\mathbf{f}_3\left(\tilde{\mathbf{q}},\dot{\tilde{\mathbf{q}}};\mu\right)=\alpha_1\begin{Bmatrix} \left(\tilde{C}_{22tt}\tilde{q}_2\tilde{q}_t^2+\tilde{C}_{23tt}\tilde{q}_3\tilde{q}_t^2+\tilde{C}_{2ttt}\tilde{q}_t^3\right) \\ \left(\tilde{C}_{33tt}\tilde{q}_3\tilde{q}_t^2+\tilde{C}_{32tt}\tilde{q}_2\tilde{q}_t^2+\tilde{C}_{3ttt}\tilde{q}_t^3\right) \\ \left(\tilde{C}_{t2tt}\tilde{q}_2\tilde{q}_t^2+\tilde{C}_{t3tt}\tilde{q}_3\tilde{q}_t^2+\tilde{C}_{tttt}\tilde{q}_t^3+\tilde{C}_{t22t}\tilde{q}_2^2\tilde{q}_t+\tilde{C}_{t33t}\tilde{q}_3^2\tilde{q}_t+\tilde{C}_{t23t}\tilde{q}_2\tilde{q}_3\tilde{q}_t\right) \end{Bmatrix}+$$

$$+\frac{3}{4}\frac{\nu}{\mu}\begin{Bmatrix} \left(C_{a2222}\dot{\tilde{q}}_2^3+C_{a2333}\dot{\tilde{q}}_3^3+C_{a2223}\dot{\tilde{q}}_2^2\dot{\tilde{q}}_3+C_{a2233}\dot{\tilde{q}}_2\dot{\tilde{q}}_3^2+\mu^3C_{a2ttt}\tilde{q}_t^3+\mu^2C_{a2tt2}\tilde{q}_t^2\dot{\tilde{q}}_2+\right. \\ \left.\mu^2C_{a2tt3}\tilde{q}_t^2\dot{\tilde{q}}_3+\mu C_{a2t22}\tilde{q}_t\dot{\tilde{q}}_2^2+\mu C_{a2t33}\tilde{q}_t\dot{\tilde{q}}_3^2+\mu C_{a2t23}\tilde{q}_t\dot{\tilde{q}}_2\dot{\tilde{q}}_3\right) \\ \left(C_{a3222}\dot{\tilde{q}}_2^3+C_{a3333}\dot{\tilde{q}}_3^3+C_{a3223}\dot{\tilde{q}}_2^2\dot{\tilde{q}}_3+C_{a3233}\dot{\tilde{q}}_2\dot{\tilde{q}}_3^2+\mu^3C_{a3ttt}\tilde{q}_t^3+\mu^2C_{a3tt2}\tilde{q}_t^2\dot{\tilde{q}}_2+\right. \\ \left.\mu^2C_{a3tt3}\tilde{q}_t^2\dot{\tilde{q}}_3+\mu C_{a3t22}\tilde{q}_t\dot{\tilde{q}}_2^2+\mu C_{a3t33}\tilde{q}_t\dot{\tilde{q}}_3^2+\mu C_{a3t23}\tilde{q}_t\dot{\tilde{q}}_2\dot{\tilde{q}}_3\right) \\ \left(C_{at222}\dot{\tilde{q}}_2^3+C_{at333}\dot{\tilde{q}}_3^3+C_{at223}\dot{\tilde{q}}_2^2\dot{\tilde{q}}_3+C_{at233}\dot{\tilde{q}}_2\dot{\tilde{q}}_3^2+\mu^3C_{atttt}\tilde{q}_t^3+\mu^2C_{attt2}\tilde{q}_t^2\dot{\tilde{q}}_2+\right. \\ \left.\mu^2C_{attt3}\tilde{q}_t^2\dot{\tilde{q}}_3+\mu C_{att22}\tilde{q}_t\dot{\tilde{q}}_2^2+\mu C_{att33}\tilde{q}_t\dot{\tilde{q}}_3^2+\mu C_{att23}\tilde{q}_t\dot{\tilde{q}}_2\dot{\tilde{q}}_3\right) \end{Bmatrix} \tag{34}$$

where $\nu=\rho_a b^2/(2m)$, and the non-dimensional coefficients $\tilde{C}_{ijhk}$ (i,j,h,k=1,2,t) are strictly related to their dimensional counterparts (see Eq. (35), Appendix A), with the inertia radii ρ substituted by their corresponding non-dimensional values $\tilde{\rho}=\rho/b$.

The linear bifurcation analysis may be carried out by writing the linearized reduced equation of motion in the state-space form (Appendix C). Appendix D illustrates the evaluation of the post-critical amplitude, based on the Multiple-Scale Method [15].

6 NUMERICAL APPLICATIONS

Preliminary numerical applications for the analysis of the aeroelastic stability of a shear-type building with external square shape are here proposed. Different layouts of the columns are considered, according to Figure 4: the position of the central columns rows is modified by varying x_{2c}- and x_{3c}-values in order to explore different eccentricity conditions. It is assumed that the uncoupled natural frequencies in the two orthogonal directions are coincident (α_{23}=1), while the torsional-to-shear frequency ratio is set $\alpha_{\theta 3}$=1.3. The non-dimensional coefficients ν and η are fixed

as ν=0.004, η=1/6; damping ratios are set as $\xi_2=\xi_3=\xi_\theta$=0.01. The mean wind velocity is assumed to be aligned with $\bar{\mathbf{a}}_2$, so that β=0. The aerodynamic coefficients for the square section are chosen according to [16] and [17] (i.e., c_d = 2.09, c_l = 0, c_m = 0, c_d' = 0, c_l' = -5.69, c_m' = 0.196, c_d'' = -18.35, c_l'' = 0, c_m'' = 0, c_d''' = 0, c_l''' = 2337, c_m''' = 130.7).

At first, the coefficients of the mechanical nonlinear terms are evaluated as functions of the position of the central row of the columns. Then, a linear bifurcation analysis is carried out and the influence on critical conditions of the non-dimensional abscissa of the central column row $\tilde{x}_{2c}$, $\tilde{x}_{3c}$ is studied. Finally, three particular column configurations are considered and the role of the mechanical and aerodynamic nonlinearities on the post-critical behavior is analyzed.

6.1 Mechanical nonlinear coefficients

Figure 5 plots values of the coefficients of the nonlinear mechanical terms as functions of the non-dimensional position of the central columns row ($\tilde{x}_{2c}=x_{2c}/b$, $\tilde{x}_{3c}=x_{3c}/b$); the constant coefficients and those linearly depending on $\tilde{x}_{2F}$ or $\tilde{x}_{3F}$ are not plotted. As observed by a direct inspection of the expression of the coefficients (Appendix A), C_{2ttt} and C_{2tt2} have the same shape as C_{3ttt} and C_{3tt3}, respectively, with C_{2ttt} and C_{2tt2} being strongly influenced by $\tilde{x}_{3c}$, C_{3ttt} and C_{3tt3} being strongly influenced by $\tilde{x}_{2c}$. The coefficients C_{2tt3} and C_{tttt} depend on both the eccentric positions $\tilde{x}_{2c}$ and $\tilde{x}_{3c}$. By comparing the numerical values of the coefficients, it can be deduced that, among the ones plotted, the most important nonlinear terms are those related to C_{2tt2} and C_{3tt3} coefficients, also for their role in the cubic coefficients appearing in the solution of the steady amplitude (Appendix D).

6.2 Bifurcation analysis

Linear bifurcation analysis is carried out by analyzing the complex eigenvalues and eigenvectors of the state-space matrix as functions of the non-dimensional mean wind velocity μ (considered as a bifurcation parameter), when the eccentricity of the central column rows $\tilde{x}_{2c}$ and $\tilde{x}_{3c}$ is varying.

Figure 6 shows the absolute value of the alongwind u_{02} (a), crosswind u_{03} (b) and torsional $u_{0\theta}$ (c) components of the critical eigenvector $\mathbf{u}_0$ as functions of $\tilde{x}_{2c}$ and $\tilde{x}_{3c}$. It clearly shows that the critical mode is, in general, a coupled vibration in the alongwind ($\bar{\mathbf{a}}_2$), crosswind ($\bar{\mathbf{a}}_3$) and torsional directions. In particular, the vibration is purely crosswind ($u_{02} = u_{0\theta} = 0$) for negligible eccentricity between the flexural and inertia center ($\tilde{x}_{2c}$ close to zero). The torsional component is mainly a function of $\tilde{x}_{2c}$, and it tends to increase on increasing $\tilde{x}_{2c}$. The alongwind component becomes remarkable for significant values of both $\tilde{x}_{2c}$ and $\tilde{x}_{3c}$ (i.e. when the lack of symmetry regards both axes). This is due to the fact that the wind acts along an axis of symmetry of the cross-section (i.e, $\beta=0$) and the alongwind component would be fully decoupled from an aerodynamic point of view.

Figure 7 shows the ratio between the critical non-dimensional mean wind velocity and the Den Hartog limit value (45) as a function of $\tilde{x}_{2c}$ and $\tilde{x}_{3c}$. It is evident that the coupling between shear and torsion has a predominant stabilizing effect, which may cause a significant increase of the critical wind velocity with respect to the classic Den Hartog criterion; this aspect is particularly relevant for high negative values of $\tilde{x}_{2c}$ and high values of $\tilde{x}_{3c}$. However, there exist some particular configurations (i.e. for $\tilde{x}_{2c}$ in the interval 0.02-0.12 and $|\tilde{x}_{3c}|>0.08$) in which the critical velocity is lower than the Den Hartog limit value: in such cases, the coupling between shear and torsion has a destabilizing effect and the traditional stability analysis which neglects such a coupling is not on the safe side.

6.3 Post-critical analysis

The post-critical analysis is carried out in the state space, assuming a small perturbation of the dimensionless mean wind velocity μ around its critical value, and applying the Multiple Scale Method (Appendix D; [11]). For the aims of this paper the stationary amplitude has been evaluated for some specific cases, in which the central columns row has been set in three different positions:

$\tilde{x}_{2c} = \tilde{x}_{3c}$ = -0.15 – configuration (a); $\tilde{x}_{2c}$ =0.15, $\tilde{x}_{3c}$ = -0.15 – configuration (b); $\tilde{x}_{2c}$ =0.02, $\tilde{x}_{3c}$ = -0.2 – configuration (c). Furthermore, the slenderness of the building and of the columns have been set λ=2.7, λ_c=10. Analyses have been carried out both taking into account and neglecting mechanical nonlinearities. Figure 8 plots the stationary amplitude of oscillations (deduced by Eq. (46) in Appendix D) for the three configurations specified. The stationary amplitude evaluated taking into account both mechanical and aerodynamic nonlinearities (solid black line – mech+aero) is compared with results obtained taking into account only aerodynamic nonlinearities (dashed black line – aero); furthermore, the post-critical amplitude for the purely-crosswind 1 degree-of-freedom galloping (solid gray line – crosswind) is reported for comparison. It can be observed that, in the case (a), Fig. 8(a), mechanical nonlinearities decrease the postcritical response amplitude in a non-negligible way. On the contrary, in the configuration (b), Fig. 8(b), the role of mechanical nonlinearities is almost negligible and the post-critical amplitude is fully dominated by aerodynamic nonlinearities. In the case (c), Fig. 8(c), a relevant reduction of the critical velocity with respect to Den Hartog limit is observed; furthermore, mechanical nonlinearities make the system stiffer, reducing the post-critical amplitude, even if terms of aerodynamic nature remain the most important ones. As a general remark, it can be observed that mechanical nonlinearities have a non-negligible effect when the coupling between shear and torsion provides a significant variation of the critical velocity. In any case, they always lead to a reduction of the postcritical amplitude.

7 CONCLUSIONS AND PROSPECTS

In this paper, a nonlinear equivalent beam model for the dynamic analysis of shear-type tower buildings has been introduced. The model allows to take into account the mechanical coupling between shear and torsion due to the lack of symmetry in the mechanical properties of the structure. This behavior leads to the appearance of nonlinear terms related to the stretching of the columns in the motion equations. This model lends itself to having applications in different fields, from wind

engineering to earthquake engineering. In the case of aeroelastic phenomena, usually dominated by the shape of the cross-section, it clearly highlights the possible influence of mechanics on aerodynamics, rarely considered.

As a first application, the analysis of the critical conditions for a square building excited by the wind along a symmetry axis has been carried out. The influence of the lack of symmetry and of the coupling between shear and torsion on the critical galloping conditions has been studied. In the case here presented, the coupling between shear and torsion has a predominant stabilizing effect, producing an increase of the critical wind velocity and a reduction of the post-critical amplitude of oscillation with respect to the purely crosswind galloping. However, there exist some specific configurations in which the coupling between shear and torsion produces a decrease of the critical velocity with respect to the purely crosswind galloping. A preliminary example on a specific class of tower buildings has shown that mechanical nonlinearities can reduce the postcritical response amplitude in a non negligible way for specific column configurations even if, in some cases, the post-critical oscillation is dominated by aeroelastic nonlinearities.

Based on the equivalent beam model here introduced, the critical wind velocity and the post-critical behavior can be estimated for different building shapes when the angle of attack of the mean wind is varying (i.e. $\beta \neq 0$). Furthermore, the influence of nonlinearities on the dynamic response to different kinds of excitation (e.g. vortex-induced actions, seismic actions) could be analyzed.

The hyperelastic law has been obtained by assuming that only columns are connecting the different floors: a generalization may be provided taking into account also the presence of shear walls and bracings in the evaluation of the equivalent stiffness terms.

Finally, the proposed equivalent beam model may be refined including a flexural deformation term and introducing an equivalent Timoshenko beam model.

ACKNOWLEDGMENTS

This work was supported by the Italian Ministry of Education, Universities and Research (MIUR) through the PRIN co-financed program 'Dynamics, Stability and Control of Flexible Structures' (grant number 2010MBJK5B).

REFERENCES

[1] A. Luongo, D. Zulli, Mathematical Models of Beams and Cables, Wiley-ISTE, 2013.

[2] A.K. Basu, G.Q. Dar, Dynamic characteristics of coupled wall-frame systems, Earthquake Engineering and Structural Dynamics, 10 (1982) 615-631.

[3] T. Balendra, S. Swaddiwudhipong, S-T. Quek, S-L, Lee, Approximate analysis of asymmetric buildings, Journal of Structural Engineering, 110(9) (1984) 2056-2072.

[4] M.J. Chajes, K.M. Romstad, D.B. McCallen, Analysis of multiple-bay frames using continuum model, Journal of Structural Engineering 119(2) (1993) 522-546.

[5] E. Miranda, S. Taghavi, Approximate floor acceleration demands in multistory buildings. I: Formulation, Journal of Structural Engineering ASCE, 131 (2005) 203-211.

[6] M. Malekinejad, R. Rahgozar, A simple analytic method for computing the natural frequencies and mode shapes of tall buildings, Applied Mathematical Modelling, 36 (2012) 3419-3432.

[7] F. Cluni, M. Gioffrè, V. Gusella, Dynamic response of tall buildings to wind loads by reduced order equivalent shear-beam models, Journal of Wind Engineering and Industrial Aerodynamics, 123 (2013) 339-348.

[8] C.P. Patrickson, P.P. Friedmann, Deterministic torsional building response to wind, Journal of the Structural Division, 105(ST12) (1979) 2621-2637.

[9] M.A.M. Torkamani, E. Pramono, Dynamic response of tall building to wind excitation, Journal of Structural Engineering ASCE, 111(4) (1985) 805-825.

[10] T. Balendra, G.K. Nathan, K.H. Kang, Deterministic model for wind-induced oscillations of buildings, Journal of Engineering Mechanics ASCE, 115(1) (1989) 179-199.

[11] G. Piccardo, F. Tubino, A. Luongo, A shear-shear torsional beam model for nonlinear aeroelastic analysis of tower buildings, Journal of Applied Mathematics and Physics (ZAMP), accepted, DOI: 10.1007/s00033-014-0456-z.

[12] F. dell'Isola, L. Rosa, C. Wozniak, Dynamics of solids with micro periodic nonconnected fluid inclusions. Arch. Appl. Mech. 67 (1997) 215–228.

[13] F. dell'Isola, L. Rosa, C. Wozniak, A micro-structured continuum modelling compacting fluid-saturated grounds: the effects of pore-size scale parameter. Acta Mech. 127(1–4) (1998) 165–182.

[14] A. Luongo, D. Zulli, Parametric, external and self-excitation of a tower under turbulent wind flow, Journal of Sound and Vibration 330 (2011) 3057-3069.

[15] A.H. Nayfeh, D.T. Mook, Nonlinear oscillations, John Wiley & Sons, 1979.

[16] Y. Nakamura, T. Mizota, Torsional flutter of rectangular prisms, Journal of the Engineering Mechanics Division, Proceedings of the American Society of Civil Engineering, 101(EM2) (1975) 125-142.

[17] T. Tamura, T. Miyagi, The effect of turbulence on aerodynamic forces on a square cylinder with various corner shapes, Journal of Wind Engineering and Industrial Aerodynamics, 83 (1999), 135-145.

[18] G. Piccardo, L.C. Pagnini, F. Tubino, Some research perspectives in galloping phenomena: critical conditions and postcritical behavior, Continuum Mechanics and Thermodynamics 27 (2015) 261-285.

[19] A. Luongo, D. Zulli, G. Piccardo, On the effect of twist angle on nonlinear galloping of suspended cables, Computers and Structures, 87 (2009) 1003-1014.

APPENDIX A. THE NONLINEAR MECHANICAL TERMS

The coefficients of the cubic mechanical terms in Eq. (23) are given by:

$$
\begin{array}{lll}
C_{2222}=3 & C_{3222}=0 & C_{t222}=-3x_{3A} \\
C_{2333}=0 & C_{3333}=3 & C_{t333}=3x_{2A} \\
C_{2ttt}=\left(7x_{3A}\rho^2-10\rho_{332}^3-10\rho_{222}^3\right) & C_{3ttt}=-\left(7x_{2A}\rho^2-10\rho_{223}^3-10\rho_{333}^3\right) & C_{tttt}=\left[10\left(\rho_{3333}^4+\rho_{2222}^4+2\rho_{2233}^4\right)-7\rho^4\right] \\
C_{2223}=0 & C_{3223}=3 & C_{t223}=3x_{2A} \\
C_{222t}=-9x_{3A} & C_{322t}=3x_{2A} & C_{t22t}=\left(3\rho_{33}^2-14x_{3A}^2+23\rho_{22}^2\right) \\
C_{2332}=3 & C_{3332}=0 & C_{t332}=-3x_{2A} \\
C_{233t}=-3x_{3A} & C_{333t}=9x_{2A} & C_{t33t}=\left(3\rho_{22}^2-14x_{2A}^2+23\rho_{33}^2\right) \\
C_{2tt2}=\left(3\rho_{33}^2-14x_{3A}^2+23\rho_{22}^2\right) & C_{3tt2}=2\left(7x_{2A}x_{3A}-10\rho_{23}^2\right) & C_{ttt2}=3\left(7x_{3A}\rho^2-10\rho_{332}^3-10\rho_{222}^3\right) \\
C_{2tt3}=2\left(7x_{2A}x_{3A}-10\rho_{23}^2\right) & C_{3tt3}=\left(3\rho_{22}^2-14x_{2A}^2+23\rho_{33}^2\right) & C_{ttt3}=-3\left(7x_{2A}\rho^2-10\rho_{223}^3-10\rho_{333}^3\right) \\
C_{223t}=6x_{2A} & C_{323t}=-6x_{3A} & C_{t23t}=4\left(7x_{2A}x_{3A}-10\rho_{23}^2\right)
\end{array}
\tag{35}
$$

being x_{2A} and x_{3A} the coordinates of the center A of the axial stiffness (Eq. (18)) and ρ the inertia radii:

$$
\begin{array}{llll}
\rho_{22}^2=\dfrac{1}{K^a}\sum_{i=1}^{N}k_i^a x_{3i}^2 & \rho_{33}^2=\dfrac{1}{K^a}\sum_{i=1}^{N}k_i^a x_{2i}^2 & \rho_{23}^2=\dfrac{1}{K^a}\sum_{i=1}^{N}k_i^a x_{3i}x_{2i} & \\
\rho_{233}^3=\dfrac{1}{K^a}\sum_{i=1}^{N}k_i^a x_{3i}x_{2i}^2 & \rho_{322}^3=\dfrac{1}{K^a}\sum_{i=1}^{N}k_i^a x_{2i}x_{3i}^2 & \rho_{222}^3=\dfrac{1}{K^a}\sum_{i=1}^{N}k_i^a x_{3i}^3 & \rho_{333}^3=\dfrac{1}{K^a}\sum_{i=1}^{N}k_i^a x_{2i}^3 \\
\dfrac{1}{K^a}\sum_{i=1}^{N}k_i^a\left(x_{2i}^2+x_{3i}^2\right)^2=\rho_{2222}^4+\rho_{3333}^4+2\rho_{2233}^4 & & &
\end{array}
\tag{36}
$$

where $K^a:=\sum_{i=1}^{N}k_i^a$ is the total axial stiffness.

It is worth pointing out the particular symmetry properties of the coefficients: $C_{3333}=C_{2222}$, $C_{3222}=C_{2333}$, $C_{3332}=C_{2223}$, $C_{3223}=C_{2332}$, $C_{3tt2}=C_{2tt3}$, $C_{t222}=3C_{222t}$, $C_{t333}=C_{333t}/3$, $C_{t223}=C_{322t}$, $C_{ttt3}=3C_{3ttt}$, $C_{ttt2}=3C_{2ttt}$, $C_{t23t}=2C_{2tt3}$, $C_{t22t}=C_{2tt2}$, $C_{t33t}=C_{3tt3}$. Furthermore, the expressions for the couples of coefficients C_{3ttt}, C_{3tt3}, C_{3tt2} can be obtained from the definitions of the coefficients C_{2ttt}, C_{2tt2} and C_{2tt3}, respectively, by substituting 2 with 3.

APPENDIX B. THE AERODYNAMIC MODEL

Aerodynamic forces are modeled based on the quasi-steady theory [18], assuming that the flow-induced forces acting on a moving cylinder can be predicted adopting the expression pertinent to a fixed cylinder in which the asymptotic flow velocity is substituted with the flow-cylinder relative velocity [19].

The approximation at the third order of the components of the aerodynamic forces in the wind reference system (drag p_{ad}, lift p_{al}, moment p_{am}, Figure 9) can be expressed as follows [11]:

$$p_{a\varepsilon}=\frac{1}{2}\rho_a b\left\{\begin{array}{l} U\left(C_{\varepsilon 2}\dot{u}_2+C_{\varepsilon 3}\dot{u}_3+UC_{\varepsilon t}\theta\right)+ \\ \left(C_{\varepsilon 22}\dot{u}_2^2+C_{\varepsilon 33}\dot{u}_3^2+U^2C_{\varepsilon tt}\theta^2+UC_{\varepsilon 2t}\dot{u}_2\theta+UC_{\varepsilon 3t}\dot{u}_3\theta+C_{\varepsilon 23}\dot{u}_2\dot{u}_3\right)+ \\ +\frac{1}{U}\left(\begin{array}{l} C_{\varepsilon 222}\dot{u}_2^3+C_{\varepsilon 333}\dot{u}_3^3+C_{\varepsilon 223}\dot{u}_2^2\dot{u}_3+C_{\varepsilon 233}\dot{u}_2\dot{u}_3^2+U^3C_{\varepsilon ttt}\theta^3+U^2C_{\varepsilon tt2}\theta^2\dot{u}_2+ \\ +U^2C_{\varepsilon tt3}\theta^2\dot{u}_3+UC_{\varepsilon t22}\theta\dot{u}_2^2+UC_{\varepsilon t33}\theta\dot{u}_3^2+UC_{\varepsilon t23}\theta\dot{u}_2\dot{u}_3 \end{array}\right) \end{array}\right\} \quad (\varepsilon=d,l,m) \tag{37}$$

where ρ_a is the air density, b is a characteristic dimension, U is the mean wind velocity and the coefficients C are given by:

$$\begin{array}{lll} C_{\varepsilon 2}=c_{\varepsilon 2}\sin\beta-2c_{\varepsilon 1}\cos\beta & C_{\varepsilon 3}=-c_{\varepsilon 2}\cos\beta-2c_{\varepsilon 1}\sin\beta & C_{\varepsilon t}=-c'_{\varepsilon 1} \\ C_{\varepsilon 22}=c_{\varepsilon 1}-c_{\varepsilon 2}\cos\beta\sin\beta+c_{\varepsilon 3}\left(\sin\beta\right)^2 & & C_{\varepsilon 33}=c_{\varepsilon 1}+c_{\varepsilon 2}\cos\beta\sin\beta+c_{\varepsilon 3}\left(\cos\beta\right)^2 \\ C_{\varepsilon tt}=\frac{1}{2}c''_{\varepsilon 1} & C_{\varepsilon 2t}=2c'_{\varepsilon 1}\cos\beta-c'_{\varepsilon 2}\sin\beta & C_{\varepsilon 3t}=2c'_{\varepsilon 1}\sin\beta+c'_{\varepsilon 2}\cos\beta \\ C_{\varepsilon 23}=c_{\varepsilon 2}\cos 2\beta-c_{\varepsilon 3}\sin 2\beta & C_{\varepsilon 222}=c_{\varepsilon 4}\left(\sin\beta\right)^3 & C_{\varepsilon 333}=-c_{\varepsilon 4}\left(\cos\beta\right)^3 \\ C_{\varepsilon 223}=-3c_{\varepsilon 4}\cos\beta\left(\sin\beta\right)^2 & C_{\varepsilon 233}=3c_{\varepsilon 4}\left(\cos\beta\right)^2\sin\beta & C_{\varepsilon ttt}=-\frac{1}{6}c'''_{\varepsilon 1} \\ C_{\varepsilon tt2}=-c''_{\varepsilon 1}\cos\beta+\frac{1}{2}c''_{\varepsilon 2}\sin\beta & C_{\varepsilon tt3}=-c''_{\varepsilon 1}\sin\beta-\frac{1}{2}c''_{\varepsilon 2}\cos\beta & C_{\varepsilon t22}=-c'_{\varepsilon 1}-c'_{\varepsilon 3}\left(\sin\beta\right)^2+c'_{\varepsilon 2}\cos\beta\sin\beta \\ C_{\varepsilon t33}=-c'_{\varepsilon 1}-c'_{\varepsilon 3}\left(\cos\beta\right)^2-c'_{\varepsilon 2}\cos\beta\sin\beta & & C_{\varepsilon t23}=-c'_{\varepsilon 2}\cos 2\beta+c'_{\varepsilon 3}\sin 2\beta \end{array} \tag{38}$$

being the coefficients $c_{\varepsilon i}$ (ε=d,l,m, i=1,..4) functions of the aerodynamic coefficients c_d, c_l, c_m, defined as follows:

$$
\begin{aligned}
c_{d1} &= c_d & c_{l1} &= c_l & c_{m1} &= c_m \\
c_{d2} &= -c_l + c_d' & c_{l2} &= c_d + c_l' & c_{m2} &= c_m' \\
c_{d3} &= -\frac{c_d}{2} - c_l' + \frac{c_d''}{2} & c_{l3} &= -\frac{c_l}{2} + c_d' + \frac{c_l''}{2} & c_{m3} &= \frac{c_m''}{2} \\
c_{d4} &= -\frac{c_l}{2} + \frac{c_d'}{6} - \frac{c_l''}{2} + \frac{c_d'''}{6} & c_{l4} &= \frac{c_d}{2} + \frac{c_l'}{6} + \frac{c_d''}{2} + \frac{c_l'''}{6} & c_{m4} &= \frac{2}{3} c_m' + \frac{c_m'''}{6}
\end{aligned}
\tag{39}
$$

where the prime symbol denotes the derivatives of the aerodynamic coefficients with respect to the instantaneous angle of attack α, evaluated at the angle of attack β.

The components (p_{a2}, p_{a3}) of the aerodynamic forces in the structural reference system ($\bar{\mathbf{a}}_2$, $\bar{\mathbf{a}}_3$) are related to the forces in the wind reference system (p_{ad}, p_{al}) through a simple rotation law (Fig. 9):

$$
\begin{aligned}
p_{a2} &= p_{ad}\cos\beta - p_{al}\sin\beta \\
p_{a3} &= p_{ad}\sin\beta + p_{al}\cos\beta
\end{aligned}
\tag{40}
$$

Thus, the components of the forces in the structural reference system p_{a2}, p_{a3} can be defined through expressions analogous to Eq. (37), (ε = 2,3), with coefficients given by:

$$
\begin{aligned}
C_{a2ijk} &= C_{dijk}\cos\beta - C_{lijk}\sin\beta \\
C_{a3ijk} &= C_{dijk}\sin\beta + C_{lijk}\cos\beta
\end{aligned}
\qquad (i,j,k=2,3,t) \tag{41}
$$

Aeroelastic forces are expressed as the sum of linear, quadratic and cubic terms, Eq. (37).

The linear terms in the velocities $\dot{u}_2$ and $\dot{u}_3$ and in the torsional rotation θ give rise to the so-called aerodynamic damping and stiffness terms, that can be collected in the corresponding matrixes $\mathbf{C}_a$ and $\mathbf{K}_a$, given by:

$$
\mathbf{C}_a = \nu \begin{bmatrix} -C_{a22} & -C_{a23} & 0 \\ -C_{a32} & -C_{a33} & 0 \\ -C_{at2} & -C_{at3} & 0 \end{bmatrix} \qquad \mathbf{K}_a = \nu \begin{bmatrix} 0 & 0 & -C_{a2t} \\ 0 & 0 & -C_{a3t} \\ 0 & 0 & -C_{att} \end{bmatrix} \tag{42}
$$

APPENDIX C. LINEAR BIFURCATION ANALYSIS

The linearized reduced equations of motion (31) can be rewritten in the following state-space form:

$$\dot{\mathbf{x}}=\mathbf{G}\mathbf{x} \tag{43}$$

$\mathbf{x}=\left\{\tilde{q}_2 \quad \tilde{q}_3 \quad \tilde{q}_t \quad \dot{\tilde{q}}_2 \quad \dot{\tilde{q}}_3 \quad \dot{\tilde{q}}_t\right\}^{\mathrm{T}}$ being the state-space vector and **G** the state-space matrix:

$$\mathbf{G}=\begin{bmatrix} \mathbf{0} & \mathbf{I} \\ -\mathbf{M}^{-1}\mathbf{K} & -\mathbf{M}^{-1}\mathbf{C} \end{bmatrix} \qquad \mathbf{C}=\mathbf{C}_s+\mu\mathbf{C}_a \qquad \mathbf{K}=\mathbf{K}_s+\mu^2\mathbf{K}_a \tag{44}$$

From Eq.(44) it should be noted that the total damping of the structure is proportional to the nondimensional wind velocity μ, which acts as a bifurcation parameter. Linear bifurcation analysis is carried out by evaluating the complex eigenvalues and eigenvectors of the state-space matrix **G** as functions of μ.

The classic Den Hartog criterion corresponds to the critical velocity μ_{DH} of the sole crosswind degree of freedom, $\tilde{q}_3$, and it is achieved when β=0 and **C**(2,2)=0:

$$\mu_{DH}=\frac{-2\xi_3}{\nu\left(c_d+c_l'\right)} \tag{45}$$

APPENDIX D. POST-CRITICAL ANALYSIS

Applying the Multiple Scales Method [15], the stationary amplitude a can be expressed as a function of $\hat{\mu}=\mu-\mu_0$ being μ_0 the critical velocity, as follows [11]:

$$a=2\sqrt{-\frac{c_{1R}}{c_{2R}}\hat{\mu}} \tag{46}$$

where c_{1R} and c_{2R} denote the real parts of the coefficients c_1 and c_2, given by:

$$\begin{aligned} c_1&=\mathbf{v}_0^{\mathrm{T}}\mathbf{G}_2\mathbf{u}_0 \\ c_2&=2\mathbf{v}_0^{\mathrm{T}}\mathbf{F}_2\left(\mathbf{u}_0,\mathbf{z}_2;\mu_0\right)+4\mathbf{v}_0^{\mathrm{T}}\mathbf{F}_2\left(\mathbf{u}_0,\mathbf{z}_0;\mu_0\right)+3\mathbf{v}_0^{\mathrm{T}}\mathbf{F}_3\left(\mathbf{u}_0,\mathbf{u}_0,\bar{\mathbf{u}}_0;\mu_0\right) \end{aligned} \tag{47}$$

In Eq. (47), $\mathbf{F}_2=\{\mathbf{0}\ \mathbf{f}_2\}^{\mathrm{T}}$, $\mathbf{F}_3=\{\mathbf{0}\ \mathbf{f}_3\}^{\mathrm{T}}$, $\mathbf{u}_0$ and $\mathbf{v}_0$ are, respectively, the right critical eigenvector and the conjugate left critical eigenvector of $\mathbf{G}_0$:

$$\mathbf{G}_0=\begin{bmatrix} \mathbf{0} & \mathbf{I} \\ -\mathbf{M}^{-1}\mathbf{K}_0 & -\mathbf{M}^{-1}\mathbf{C}_0 \end{bmatrix} \qquad \mathbf{K}_0=\mathbf{K}_s+\mu_0^2\mathbf{K}_a \qquad \mathbf{C}_0=\mathbf{C}_s+\mu_0\mathbf{C}_a \tag{48}$$

Furthermore, $\mathbf{G}_2$ is defined as follows:

$$\mathbf{G}_2=\begin{bmatrix} \mathbf{0} & \mathbf{0} \\ -\mathbf{M}^{-1}\mathbf{K}_2 & -\mathbf{M}^{-1}\mathbf{C}_2 \end{bmatrix} \qquad \mathbf{K}_2=2\mu_0\mathbf{K}_a \qquad \mathbf{C}_2=\mathbf{C}_a \tag{49}$$

Finally, $\mathbf{z}_0$ and $\mathbf{z}_2$ are solutions of the following equations:

$$\begin{aligned} \left(2i\omega\mathbf{I}-\mathbf{G}_0\right)\mathbf{z}_2&=\mathbf{F}_2\left(\mathbf{u}_0,\mathbf{u}_0;\mu_0\right) \\ -\mathbf{G}_0\mathbf{z}_0&=\mathbf{F}_2\left(\mathbf{u}_0,\bar{\mathbf{u}}_0;\mu_0\right) \end{aligned} \tag{50}$$

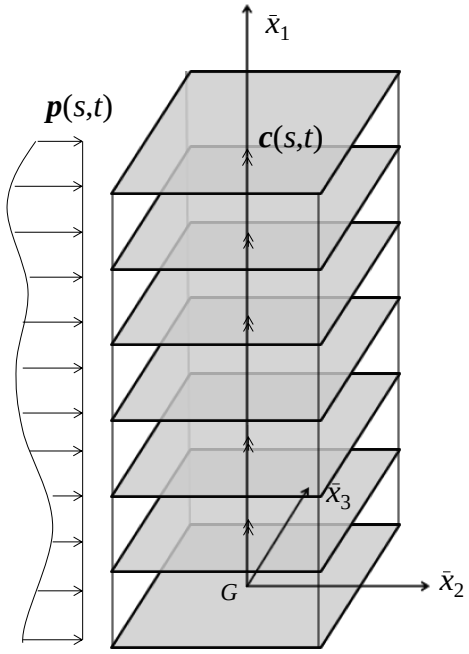

Figure 1. Tower building configuration and external loading.

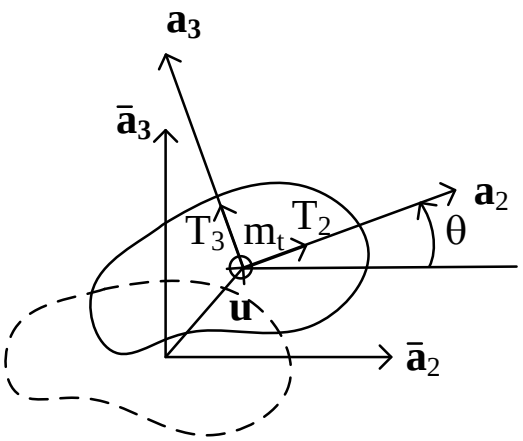

Figure 2. Tower building: reference and current bases, configuration variables and internal forces.

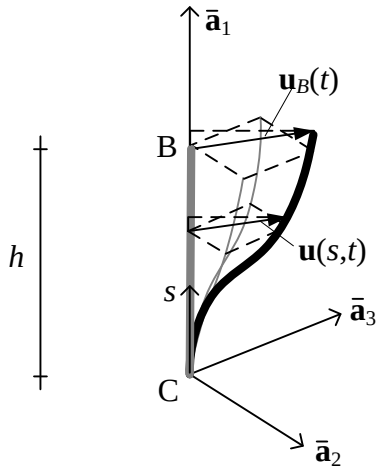

Figure 3. Single column deformation.

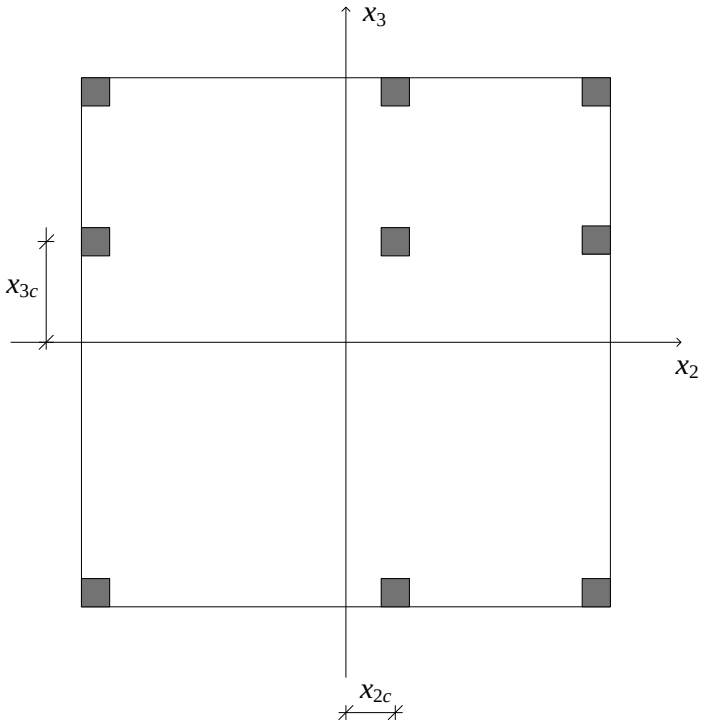

Figure 4: Numerical example: non-symmetric layout of the columns

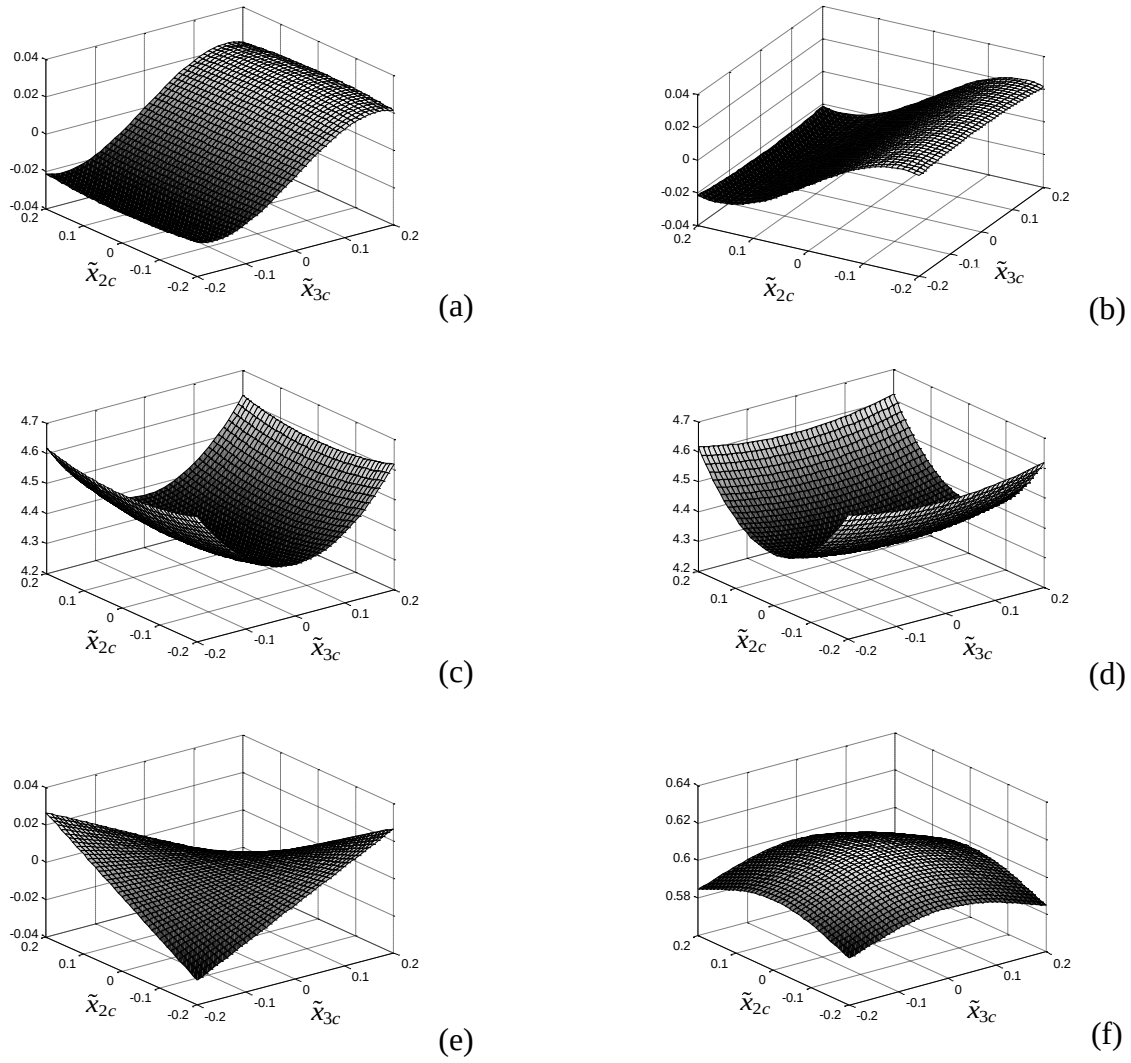

Figure 5: Coefficients of nonlinear mechanical terms:

(a) C_{2ttt}, (b) C_{3ttt}, (c) C_{2tt2}, (d) C_{3tt3}, (e) C_{2tt3}, (f) C_{tttt}.

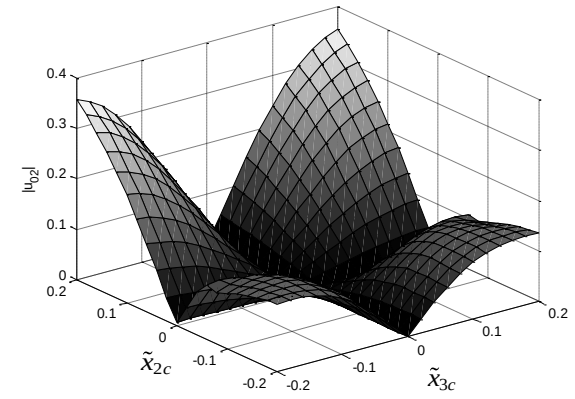

(a)

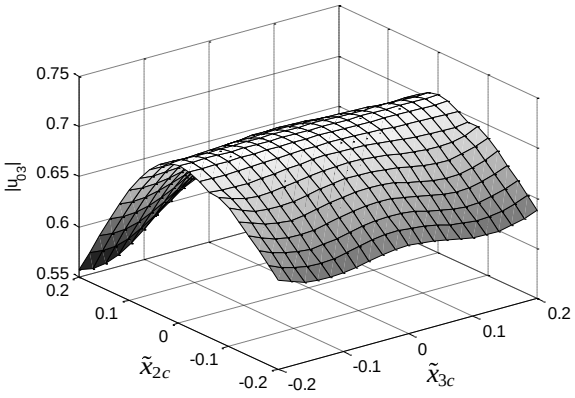

(b)

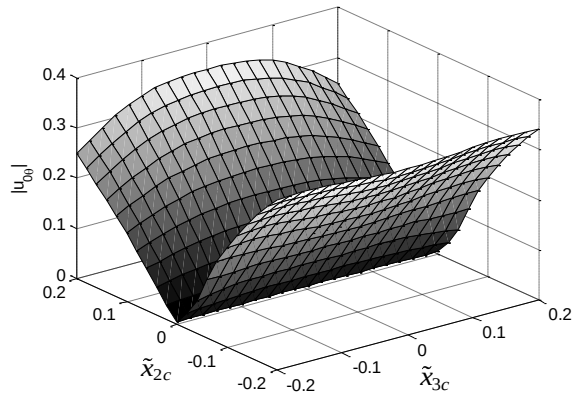

(c)

Figure 6: Components of the critical mode.

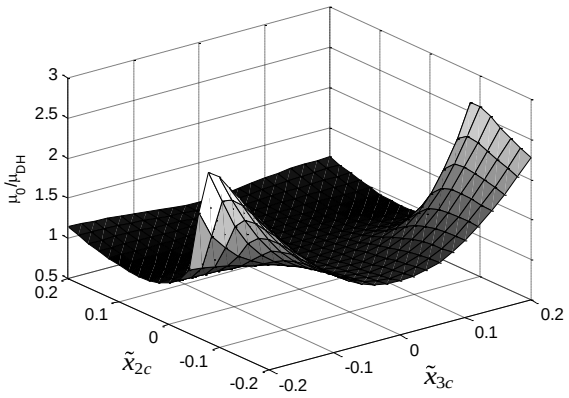

Figure 7: Critical mean wind velocity (non-dimensional with respect to Den Hartog limit).

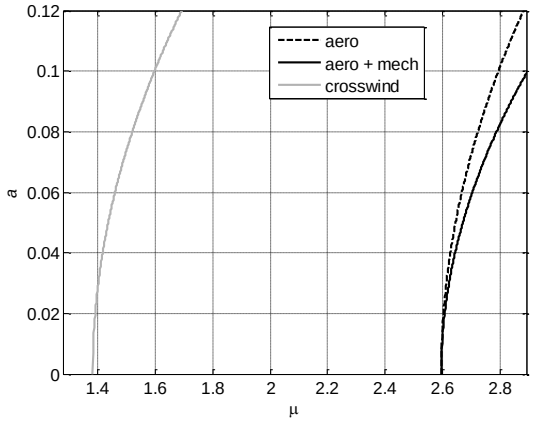

(a)

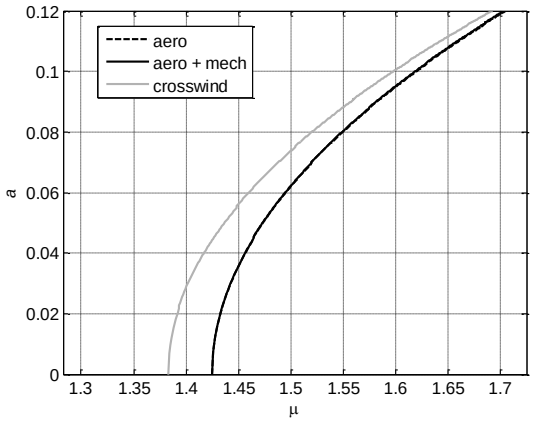

(b)

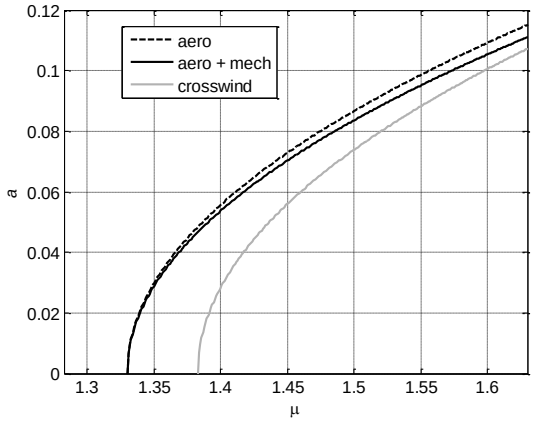

(c)

Figure 8: Post-critical amplitude: relative importance of aerodynamic and mechanical nonlinearities: $\tilde{x}_{2c} = \tilde{x}_{3c}$ =-0.15 – configuration (a); $\tilde{x}_{2c}$ =0.15, $\tilde{x}_{3c}$ =-0.15 – configuration (b); $\tilde{x}_{2c}$ =0.02, $\tilde{x}_{3c}$ =-0.2 – configuration (c) .

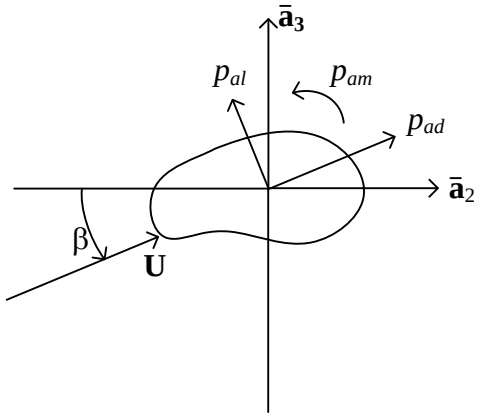

Figure 9: Aerodynamic force components